Original Article

Involvement of STAT3 in Bladder Smooth Muscle Hypertrophy Following Bladder Outlet Obstruction

Osamu Fujita[a], Masato Asanuma[b], Teruhiko Yokoyama[a]*,
Ikuko Miyazaki[b], Norio Ogawa[b], and Hiromi Kumon[a]

Departments of [a]Urology, and [b]Brain Science, Okayama University Graduate School of Medicine,
Dentistry and Pharmaceutical Sciences, Okayama 700–8558, Japan

We examined the involvement of the signal transducer and activator of transcription 3 (STAT3) in bladder outlet obstruction (BOO)-induced bladder smooth muscle hypertrophy using a rat *in vivo* and *in vitro* study. BOO induced increases in bladder weight and bladder smooth muscle thickness 1 week after the operation. By using antibody microarrays, 64 of 389 proteins blotted on the array met our selection criteria of an INR value between ≥ 2.0 and ≤ 0.5. This result revealed up-regulation of transcription factors, cell cycle regulatory proteins, apoptosis-associated proteins and so on. On the other hand, down-regulation (INR value ≤ 0.5) of proteins was not found. In a profiling study, we found an increase in the expression of STAT3. A significant increase in nuclear phosphorylated STAT3 expression was confirmed in bladder smooth muscle tissue by immunohistochemistry and Western blot analysis. Cyclical stretch-relaxation (1 Hz) at 120% elongation significantly increased the expression of STAT3 and of α-smooth muscle actin in primary cultured bladder smooth muscle cells. Furthermore, the blockade of STAT3 expression by the transfection of STAT3 small interfering RNA (siRNA) significantly prevented the stretch-induced increase in α-smooth muscle actin expression. These results suggest that STAT3 has an important role in the induction of bladder smooth muscle hypertrophy.

Key words: benign prostatic hyperplasia, bladder outlet obstruction, bladder smooth muscle, signal transducer and activator of transcription 3 (STAT3), small interfering RNA (siRNA)

Bladder outlet obstruction (BOO), such as benign prostatic hyperplasia (BPH), is a common disorder, affecting 50% to 80% of males over the age of 50 [1]. It causes various urinary symptoms; it leads to irritability, urgency, urge incontinence due to detrusor hyperreflexia in the storage phase, hesitancy and weak flow in the voiding phase

with consequent retention in the end phase. Furthermore, BOO causes compensatory bladder smooth muscle hypertrophy that aggravates various urinary dysfunctions [1]. Previous studies show that BOO increases the activation of some molecules in the bladder smooth muscle, for example, nuclear factor κB (NF-κB) [2], c-Jun NH2-terminal kinase (JNK) [3], cyclooxygenase-2 (COX-2) [4], basic fibroblast growth factor (bFGF) [5] and calcineurin [6]. However, the cellular and molecular mechanisms of BOO-induced bladder smooth muscle hyper-

trophy are still obscure.

Antibody microarray provides a powerful analytical technique for high-throughput profiling protein expression. It is useful for screening protein expression by measuring expression levels of abundant proteins simultaneously and semi-quantitatively with a single experiment [7]. To elucidate molecular events involved in bladder smooth muscle hypertrophy following BOO, protein expression was profiled in the bladder tissue of a rat BOO model that showed smooth muscle hypertrophy by using antibody microarrays as a preliminary screening study. Among the molecules up-regulated by BOO in the antibody microarray assay, we focused on the role of the signal transducer and activator of transcription 3 (STAT3) that is related to inflammatory reaction and cytokine signals. In the present study, we examined the involvement of STAT3 in bladder smooth muscle hypertrophy using an *in vivo* BOO model, and we examined mechanical stretch stress on primary cultured bladder smooth muscle cells by inhibiting STAT3 expression through transfection of its small interfering RNA (siRNA).

Materials and Methods

Surgical induction of rat BOO models.   All animal procedures described in this report were in strict accordance with the National Institutes of Health Guide for the Care and Use of Laboratory Animals (NIH, Bethesda, MD, USA) and with the Guideline for Animal Experiments of Okayama University Advanced Science Research Center. The partial BOO rat model was prepared by a previously described procedure [6]. Eight-week-old female Sprague-Dawley rats weighing 180 to 200 g were used in the surgical induction of rat BOO models. The rats were sacrificed 1 week after the surgery to remove the whole bladder. After observation and weighing, the bladder tissue was used in the following experiments.

Protein extraction from bladder tissue. The bladder mucosa was removed from the bladder tissue with a pair of scissors, and then the remaining tissue, including bladder smooth muscle, was frozen in liquid nitrogen. The frozen tissue was broken with a hammer. The samples were homogenized with 300 μl of ice-cold RIPA buffer (50 mM Tris-HCl (pH

7.5), 250 mM sucrose, 75 mM urea, 60 mM β-mercaptoethanol, 5% sodium dodecyl sulfate (SDS)) plus a proteinase inhibitor using a Polytron homogenizer (model PT 1200) at maximum speed for 6 bursts of 10–30 sec each. After incubation on ice for 30 min, the homogenates were centrifuged (16,000 g × 20 min at 4 ℃), and then the supernatants were obtained as total cell lysates. The protein concentration of lysates was measured by protein assay reagents (RC DC Protein Assay reagents; Bio-Rad Laboratories, Hercules, CA, USA).

Antibody microarray.   Protein lysate labeling with fluorescent dye and protein expression profiling were performed using antibody microarrays (BD Clontech Ab Microarray 380, #K1847–1, BD Biosciences Clontech, Palo Alto, CA, USA) according to the manufacturer's instructions. Each 450 μl of 1.1 mg/ml protein lysate from the bladder after BOO or sham operation was labeled with 50 μl of Cy3 or Cy5 fluorescent dye (Amersham Biosciences, Arlington Heights, IL, USA) with incubation at 4 ℃ for 90 min. Each antibody microarray glass slide was incubated with either of the labeled protein mixtures (BOO-Cy5 + sham-Cy3 or sham-Cy5 + BOO-Cy3) at room temperature for 30 min. The Cy5/Cy3 fluorescent signal ratios for all coordinates on each array (ratio BOO-Cy5/sham-Cy3 or ratio sham-Cy5/BOO-Cy3) were calculated with array analysis software (GenePix Pro). The change in the protein expression of each coordinate on the array was evaluated by the internally normalized ratio (INR): the square root of (ratio BOO-Cy5/sham-Cy3)/(ratio sham-Cy5/BOO-Cy3).

Primary culture of rat bladder smooth muscle cells.   Under deep sodium pentobarbital anesthesia (80 mg/kg, i.p.), the bladder was removed from female Sprague-Dawley rats (10 weeks of age) and rinsed with 10 mM phosphate buffered saline (PBS). After the urothelium was removed, the bladder was incubated with 0.2% trypsin in RPMI-1640 medium (Invitrogen, Carlsbad, CA, USA) for 30 min at 37 ℃. After centrifugation for 5 min at 2,000 rpm, the precipitated bladder was minced into small pieces. The minced bladder tissue was incubated with 0.1% collagenase in RPMI-1640 medium for 30 min at 37 ℃ and centrifuged for 5 min at 2,000 rpm, after which the pellet was suspended into culture medium RPMI-1640 containing 10% fetal bovine

serum, 1% penicillin and streptomycin. The cells ($5,000$ cells/mm^2) were seeded in culture dishes and cultured in the culture medium in a humidified 5% CO2–95% air atmosphere at 37 °C.

Application of cyclical stretch-relaxation to cultured bladder smooth muscle cells. Cultured bladder smooth muscle cells were removed from the dish with 0.02% trypsin in PBS and were transferred onto a 10.24 cm^2 collagen-coated silicone chamber at a density of 5×10^5 cells/cm^2 in the culture medium. The silicon chamber had a 200-μm-thick transparent bottom center, and the bottom corner was 400 μm thick to prevent narrowing at its bottom center. The silicone chamber was attached to a cell-stretching apparatus (NS-500, Strex, Nagoya, Japan) that was driven by a computer-controlled stepping motor. After cells were allowed to attach to the chamber bottom for 24 h, a uni-axial sinusoidal stretch (120% peak to peak, at 1 Hz) was applied at 37 °C in a humidified 5% CO2–95% air atmosphere. Attached bladder smooth muscle cells were subjected to stretch/relaxation for various durations up to 24 h.

Blocking STAT3 expression by RNA inter-ference methods. To examine the effects of inhibiting STAT3 expression on bladder smooth muscle hypertrophy, RNA interference for STAT3 was performed on cultured bladder smooth muscle cells attached to the silicone chamber in advance of the stretch stimuli using the Silencer siRNA Transfection Kit (Ambion, Austin, Texas, USA) according to the manufacturer's instructions. Before the siRNA transfection, bladder smooth muscle cells plated on a collagen-coated silicone chamber at a density of 5×10^5 cells/cm^2 were cultured in culture medium with 10% fetal bovine serum. The siRNA for STAT3 (Silencer Validated siRNA STAT3, Ambion, Austin, Texas, USA) at a final concentration of 100 nM pre-incubated with siPORT Lipid (Ambion) in serum-free medium for 20 min was added onto the cells and then incubated in culture medium for another 1 h to transfect the siRNA. After the addition of fresh culture medium to the serum, cells were cultured for 24 h and then challenged with the cyclical stretch relaxation described above. Scrambled control siRNA having no significant homology to rat gene sequences were used as negative control siRNA in the present study.

Protein extraction from cultured bladder smooth muscle cells. Cultured bladder smooth muscle cells after the stretch were washed with 10 mM PBS and then lysed in 100 μl of ice-cold RIPA buffer 1 mM PBS (pH 7.4), 1% Nonidet P-40, 0.5% sodium deoxycholate, 0.1% SDS plus a proteinase inhibitor (0.1 mg/ml phenylmethylsulfonyl fluoride). After incubation on ice for 60 min, the homogenates were centrifuged ($16,000$ g $\times 20$ min at 4 °C), and then the supernatants were obtained as total cell lysates.

Western blot analysis. Western blot analysis was performed as described previously [6, 8]. The total cell lysate (50 μg) from the samples was mixed with the sampling buffer (4% SDS, 0.02% bromophenol blue, 20% glycerol, and 10% β-mercaptoethanol in 125 mM Tris-HCl, pH 6.8) and boiled. The proteins were separated on 10% or 12.5% SDS-polyacrylamide gels. Blots were incubated with mouse monoclonal antibodies against STAT3 (diluted 1:2,500; BD Biosciences), α-smooth muscle actin (1:400; Sigma-Aldrich, St. Louis, MO, USA), glyceraldehyde-3-phosphate dehydrogenase (GAPDH, 1:100; Chemicon, Temecula, CA, USA), rabbit polyclonal anti-phospho-STAT3 (Tyr705) antibody (diluted 1:1,000 in PBST; Cell Signaling Technology, Boston, MA, USA), anti-NF-κB antibody (1:200; Santa Cruz Biotechnology, Santa Cruz, CA, USA), anti-phospho-NF-κB p65 (Ser536) antibody (diluted 1:1,000 in PBST; Cell Signaling Technology), and bFGF (1:500; R&D Systems, Minneapolis, MN, USA). The blots were then reacted with donkey anti-mouse IgG (Chemicon).

Morphological observation of bladder tissue slice. One week after the surgical induction of BOO models, rats were transcardially perfused with saline followed by a fixative containing 4% paraformaldehyde and 0.35% glutaraldehyde in 0.1 M phosphate buffer (PB, pH 7.4) under deep anesthesia. After the perfusion, the whole bladder was removed, post-fixed for 24 h in a fixative containing 4% paraformaldehyde in 0.1 M PB (pH 7.4), and then cryoprotected in 15% sucrose in PB for 48 h. The bladder tissue frozen with powdered dry ice was cut into 10-μm-thick slices by a cryostat. Some slices of bladder tissue were fixed and stained with hematoxylin-eosin. The thickness of the bladder wall and smooth muscle layer was evaluated using computer-

ized image analysis software (NIH Image 1.56) run on a Macintosh computer. Within each bladder slice, the smooth muscle layer was outlined with a screen cursor driven by a hand-held mouse. Relative size units were then measured.

For the immunohistochemistry of phosphorylated STAT3, the sections were soaked in 0.5% H_2O_2 in 10 mM PBS containing 0.2% Triton X-100 (PBST) for 30 min and then incubated in 1% normal goat serum in PBST for 30 min at room temperature. After washing with PBST (3×10 min), the sections were exposed to anti-phospho-STAT3 (Tyr705) rabbit polyclonal antibody (diluted 1:100 in PBST; Cell Signaling) for 18 h at 4 ℃. After incubation with the primary antibody, sections were washed for 5×5 min in PBST before being incubated with biotinylated goat anti-rabbit IgG secondary antibody (diluted 1:200 in PBST: Vector Laboratories, Burlingame, CA, USA) for 2 h at room temperature. Following washes in PBST (3×10 min), the sections were incubated with the avidin-biotin peroxidase complex (diluted 1:250) for 1 h. Phosphorylated STAT3-immunopositive cells were visualized by 3,3′-diaminobenzidine, nickel, and H_2O_2 and counterstained with eosin. Phosphorylated STAT3-immunoreactive cells in the bladder section were counted manually on 16–18 slices per group using a microscope at a magnification of X200 with a superimposed grid. Counting was performed blindly.

Immunohistochemistry of cultured bladder smooth muscle cells. Immunohistochemistry of cultured bladder smooth muscle cells was performed as described previously [6]. Briefly, cultured bladder smooth muscle cells after the stretch stimuli on the silicone chamber were fixed with 4% paraformaldehyde in 0.1 M phosphate buffer. The cell culture chambers were incubated with mouse monoclonal anti-α-smooth muscle actin primary antibody (diluted 1:200; Sigma-Aldrich). After a wash, the cell samples were reacted with fluorescein isothiocyanate (FITC)-conjugated secondary antibodies (diluted 1:200; Chemicon). Immunofluorescence signals were analyzed under a fluorescence microscope (BX50-FLA, Olympus, Tokyo, Japan). The relative density of the immunofluorescence signals was assessed using the microscope at a magnification of X400 and Macintosh computer-based image analysis systems (NIH Image 1.56).

Statistical analyses. Results are given as means $\pm$ SEM values. Statistical analyses of the data were performed using Student's t-test or one-way analysis of variance (ANOVA) followed by post-hoc Fisher's PLSD test. A p value less than 0.01 denoted the presence of a statistically significant difference.

Results

Bladder weight and morphological change in the bladder smooth muscle in rat BOO model. BOO induced a marked increase in bladder weight (BOO, 215.8 ± 24.8 mg ranging from 118 to 335 mg vs. controls, 60.5 ± 5.11 mg ranging from 30 to 77 mg) at 1 week after the operation (Fig. 1A). Histological observation revealed an increase in the thickness of the bladder smooth muscle layer 1 week after BOO, although there was no infiltration of connective tissue or inflammatory cells among the muscle cells (Fig. 1B).

Antibody microarrays. As a preliminary screening, we performed a profiling of BOO-induced protein expression in the bladder smooth muscle by using the antibody microarray. When protein expression in the rat bladder tissue was screened 1 week after BOO by using antibody microarrays, 64 of 389 proteins blotted on the array met our selection criteria, which was an INR value between ≥ 2.0 and ≤ 0.5. The antibody microarray approach revealed up-regulation of transcription factors, cell cycle-regulatory proteins, apoptosis-associated proteins, cytoskeletal proteins, adhesion molecules, growth factor- and stress-related proteins, signal transduction-related proteins, and nitric oxide-related proteins in the bladder tissue 1 week after the BOO operation (Table 1). To a lesser extent, NF-κB and Fos (AP-1) were also up-regulated. INR values were 1.85 and 1.25, respectively.

Changes in STAT3, bFGF, NF-κB, and α-smooth muscle actin expression in smooth muscle after BOO. In the profiling study using the antibody microarray, we found a marked increase in the expression of acute phase response factor STAT3 in rat bladder smooth muscle tissue after the BOO operation. In the present study, therefore, we focused on the involvement of the inflammatory factor STAT3 in bladder smooth muscle hypertrophy

following BOO. Immunohistochemistry of STAT3 in rat bladder sections showed marked and constitutive expression of phosphorylated STAT3 (activated form) in the nuclei of bladder mucosal epithelial cells of both control and BOO animals (Fig. 1C). The apparent expression of the nuclear phosphorylated STAT3 was revealed 1 week after BOO, although there was little induction of STAT3 in the bladder smooth muscle cells of the sham-operated control group (Fig. 1C). The number of phosphorylated STAT3-immunopositive cells significantly increased

in the bladder smooth muscle layer of BOO rats, compared with sham-operated controls (Fig. 1D).

In Western blot analysis, significant increases in the expression of STAT3 and its activated form of phosphorylated STAT3 were confirmed in the lysate from rat bladder smooth muscle tissue 1 week after BOO (Fig. 2A & 2B). This is consistent with the antibody array results. It was also revealed that the expression of bFGF, NF-κB, and its activated form, phosphorylated NF-κB p65, all of which were previously reported to be elevated following BOO [2, 5],
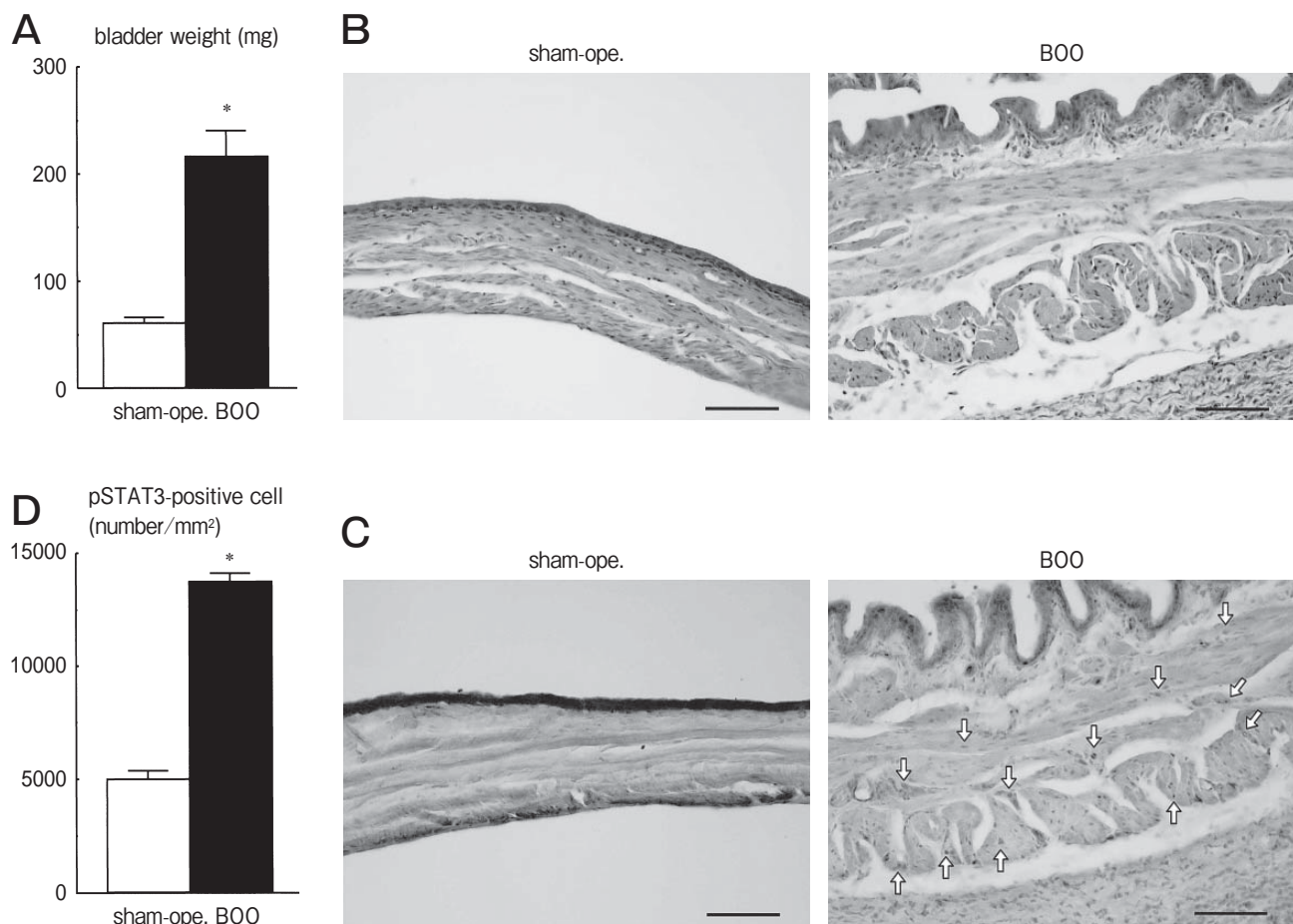
Fig. 1   Smooth muscle hypertrophy and histological changes after partial BOO. **A**, Changes in bladder weight 1 week after BOO. Value shows mean bladder weight ± SEM in 10 rats per group. *$p < 0.01$ vs. sham-operated control group; **B**, Morphological changes in bladder section 1 week after the operation in sham-operated control group and BOO group (hematoxylin-eosin staining). Scale bar indicates 50 μm; **C**, Immunohistochemistry of phosphorylated STAT3 in bladder slice 1 week after BOO with light eosin counterstaining. Dark gray signals (arrows) are representative phosphorylated STAT3-immunopositive nuclei. Scale bar = 50 μm; **D**, Quantitative analysis of number of phosphorylated STAT3-immunopositive cells in the bladder smooth muscle layer after BOO. Value shown is the mean number of phosphorylated STAT3-immunopositive cells ± SEM (number/mm^2 on 16–18 slices/group). *$p < 0.01$ vs. sham-operated control group.

Table 1　Profiling of protein expression in the bladder tissue 1 week after BOO by using antibody microarray.

Up-regulated proteins which corresponding INR values on the array were ≥2.0 were evaluated the proteins were more abundant in BOO group than sham-operated group.

| Category/Protein	INR	Swiss Prot	Function
Transcription factors			
E2F-1	2.15	Q01094	Transcription factor as a determinant of the G1/S-phase transition
STAT3	2.10	P40763	Signal transducer and activator of transcription 3 (Acute-phase response factor)
M33	2.10	P30658	Chromatin regulator
Per2	2.08	O15055	Regulate the circadian cycle via transcriptional control
TF II -1/BAP-135	2.07	O15359	General transcription factor II-I (GTFII-I) (TFII-I) (Bruton tyrosine kinase-associated protein-135) (BTK-associated protein-135) (BAP-135)
IKKγ/3/NEMO	2.04	Q9Y6K9	NF-κB essential modulator
IKKα/1	2.04	O15111	Inhibitor of NF-κB kinase alpha subunit
LXR	2.00	Q13133	Orphan receptor regulation of cholesterol homeostasis
Cell cycle regulatory proteins			
CDC27	2.30	P30260	Cell division cycle protein 27 homolog
AIM-1	2.21	C60446	Serine/threonine protein kinase 12
SRPK1	2.17	Q12890	Phosphorylation of SR proteins during the cell cycle
DBP2	2.15	O60231	Putative pre-mRNA splicing factor RNA helicase
DNA polymerase δ	2.15	P28340	DNA polymerase delta catalytic subunit as polymerase and exonuclease
cdk1	2.10	P06493	Control of the eukaryotic cell cycle
XIN	2.08	Q8TCG7	Hypothetical protein
NEK2	2.06	P51955	Serine/threonine-protein kinase NEK2
CDC25 C	2.00	P30307	Dosage-dependent inducer in mitotic control
Cyclin D1	2.00	P24385	Essential for the control of the cell cycle at the G1/S (START) transition
Apotosis-associated proteins			
Caspase7/Mch3	2.41	P55210	Caspase-7 precursor (ICE-like apoptotic protease 3) (ICE-LAP3)
DDX1	2.15	Q92499	ATP-dependent helicase DDX1
MEK 5	2.08	Q92961	Mitogen-activated protein kinase kinases
GOK/Stim1	2.06	Q13586	Stromal interaction molecule 1 precursor as possible adhesion molecule in early hematopoiesis
IKKγ/3/NEMO	2.04	Q9Y6K9	NF-κB essential modulator
IKKα/1	2.04	O15111	Inhibitor of NF-κB kinase alpha subunit
XPA	2.02	P23025	DNA-repair protein complementing XP-A cells
hILP/XIAP	2.02	P98170	Apoptotic suppressor. Inhibitor of caspase-3, -7 and -9
Ku-80	2.00	P13010	Single stranded DNA-dependent ATP-dependent helicase
Oncogenes & tumor suppressors			
c-Myc	2.09	P01106	Myc proto-oncogene protein in the regulation of gene transcription, especially growth-related gene transcription
erbB-2/HER-2	2.08	P04626	Receptor protein-tyrosine kinase erbB-2 precursor (C-erbB-2) (Tyrosine kinase-type cell surface receptor HER2) (MLN 19)
eIF-5	2.03	P55010	Eukaryotic translation initiation factor 5
eIF-4γ	2.02	Q04637	Eukaryotic translation initiation factor 4 g
HPV-16 L1	2.01	P03101	Human papillomavirus type 16
Cytoskeletal proteins			
Myogenin	2.08	P15173	Myogenic factor Myf-4 involved in muscle differentiation
Cypher1	2.05	O75112	Adaptor that couples PKC-mediated signaling to the cytoskeleton in striated muscle
Tensin	2.04	Q9HBL0	Influenced actin filament organization
Moesin	2.04	P26038	Involved in connections of major cytoskeletal structures to the plasma membrane
ABP-280	2.02	P21333	Endothelial actin-binding protein
MAP4	2.01	P27816	Non-neuronal microtubule-associated protein
Myr6	2.01	Q9ULV0	Myosin Vb
SCP3	2.00	P70281	Component of the transverse filaments of synaptonemal complexes

Category/Protein	INR	Swiss Prot	Function
Adhesion molecules			
Fibronectin	2.09	P02751	Role in cell adhesion, morphology, and surface architecture
Cadherin-5	2.09	P33151	Calcium dependent cell adhesion protein
Kalinin B1	2.05	Q13751	Binding to cells via a high affinity receptor
Neuroglycan C	2.01	O95196	Neural transmembrane chondroitin sulfate proteoglycan
Growth factor- & stress-related proteins			
HAX-1	2.15	O00165	HS1-binding protein
HS1	2.11	P14317	Substrate of the antigen receptor-coupled tyrosine kinase
TGF-β1	2.10	P01137	Transforming growth factor β1 precursor that controls proliferation and differentiation
COX-2/PGHS	2.04	P35354	Prostaglandin G/H synthase 2 precursor
Neuropilin-2	2.02	O60462	Vascular endothelial cell growth factor 165 receptor 2
Signal transduction-related proteins			
AIM-1	2.21	C60446	Serine/threonine protein kinase 12
SRPK1	2.17	Q12890	Phosphorylation of SR proteins during the cell cycle
AKAP149	2.11	Q92667	A-kinase anchor protein 149 kDa that anchors regulatory subunits of protein kinase A to the mitochondorial outer membrane
Rho-GDI	2.11	P52565	Regulate the GDP/GTP exchange reaction of the Rho proteins
CaM Kinase Kinase	2.10	Q9BQH3	Upstream regulator in the Ca^{2+}/CaM-dependent neural processes
Calretinin	2.10	P22676	Promote calcium homeostasis by acting as buffers of intracellular Ca^{2+}
MEK 5	2.08	Q92961	Mitogen-activated protein kinase kinases
erbB-2/HER-2	2.08	P04626	Receptor protein-tyrosine kinase erbB-2 precursor (C-erbB-2) (Tyrosine kinase-type cell surface receptor HER2) (MLN 19)
NEK2	2.06	P51955	Serine/threonine-protein kinase NEK2
SPA-1	2.04	O60484	Signal-induced proliferation-associated protein 1; GTPase activator for the nuclear Ras-related regulatory proteins Rap1 and Rap2
CPG16/CaM Kinase VI	2.02	O15075	Serine/threonine-protein kinase DCAMKL1 (Doublecortin-like and CAM kinase-like 1) that may be involved in a calcium-signaling pathway
IQGAP1	2.02	P46940	Bind to activated CDC42 and associate with calmodulin
NO-related proteins			
iNOS/TYPE II	2.10	P35228	Inducible nitric oxide synthase (iNOS)
nNOS	2.08	P29475	Neuronal nitric-oxide synthase, brain (nNOS)
Arginase I	2.01	P05089	Catalyze the last step of Urea cycle; Arginine metabolism (Liver type)
Nuclear			
DDX1	2.15	Q92499	ATP-dependent helicase DDX1
AF6	2.11	P55196	Chromosomal translocation
Chromogranin A	2.05	P10645	Protein costored and coreleased with catecholamines
XPA	2.02	P23025	DNA-repair protein complementing XP-A cells
Organelle			
SNX2	2.10	O60749	Interact with a variety of receptor types in protein transport
GM130	2.06	Q9NYF9	Golgi structural protein
ERp72	2.01	P13667	Protein disulfide isomerase A4 precursor
Neuroscience			
SH2-B	2.13	Q9NRF1	Signaling molecules in tyrosine kinase receptor pathways
Apo E	2.11	P02649	Main apoprotein of the chylomicron

was significantly increased after the BOO operation (Fig. 2A & 2B). The expression of α-smooth muscle actin, which is known as a specific protein in smooth muscle, also significantly increased following BOO (Fig. 2A & 2B).

Changes in STAT3 and α-smooth muscle actin expression in bladder smooth muscle cells after cyclical stretching and effects of transfection of siRNA for STAT3.   Changes in the STAT3 expression in primary cultured bladder smooth muscle cells were examined during the stress of cyclical stretching. Western blot analysis revealed that STAT3 expression was significantly increased by a 3-h stretch compared with non-stretched controls. The expression gradually decreased from the 6-h to the 24-h stretch. In contrast, α-smooth muscle actin expression gradually increased from the 3-h to the 24-h stretch (Fig. 3A & 3B).

The STAT3 expression was greatly reduced by the transfection with STAT3 siRNA, but not with the scrambled control siRNA (Fig. 4A). The transfection reagent or scrambled control siRNA showed no effects on cell viability in the present study (data not shown). Immunohistochemical study revealed that α-smooth muscle actin was strongly expressed in cultured bladder smooth muscle cells after the 24-h stretch compared with that in non-stretched controls (Fig. 4B). Interestingly, the transfection of STAT3 siRNA significantly inhibited the increase of α-smooth muscle actin expression induced by the 24-h stretch (Fig. 4B & 4 C), although the transfection with control siRNA showed no effects of the stretch-induced increase in α-smooth muscle actin.
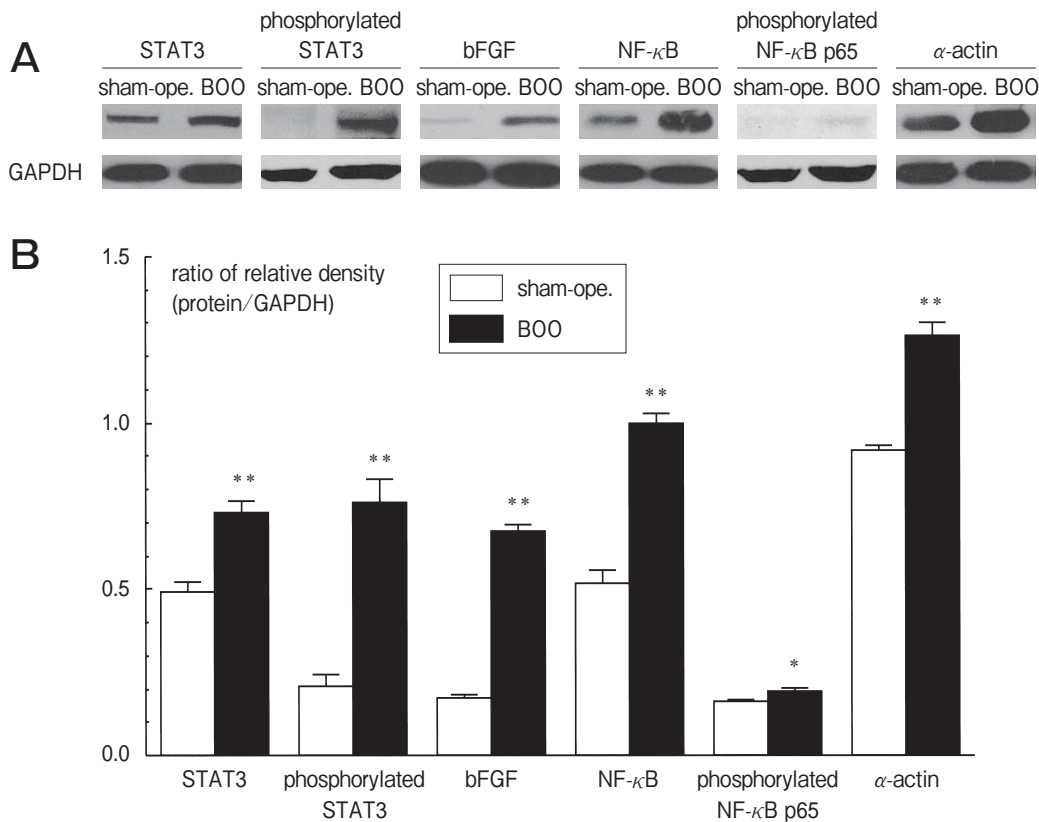

Fig. 2   Changes in STAT3, bFGF, NF-κB, and α-smooth muscle actin expression in bladder smooth muscle after BOO. Representative Western blots for STAT3, phosphorylated STAT3, bFGF, NF-κB, phosphorylated NF-κB p65, and α-smooth muscle actin, and corresponding signals of GAPDH (**A**). Quantitative analyses of the relative density of detected signals on the blots for STAT3, phosphorylated STAT3, bFGF, NF-κB, phosphorylated NF-κB p65, and α-smooth muscle actin (**B**). The value is the mean of the ratio for each detected protein/GAPDH (relative density) $\pm$ SEM. $*p < 0.05$, $**p < 0.01$ vs. sham-operated control group.

A

B
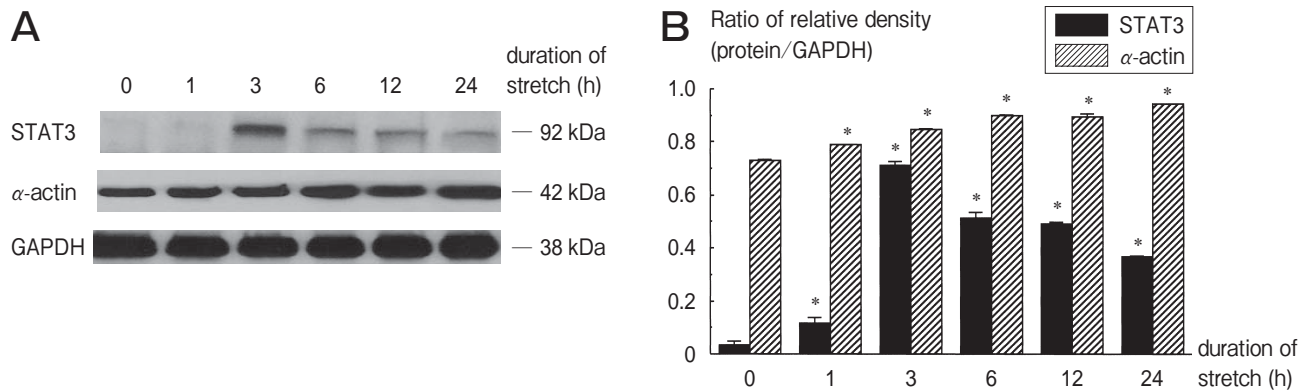
Fig. 3   Changes in STAT3 and α-smooth muscle actin expression in bladder smooth muscle cells after cyclical stretching. Representative Western blots for STAT3 and α-smooth muscle actin (**A**). Quantitative data of STAT3 and α-smooth muscle actin expression (**B**). Values are means of the ratio for each detected protein/GAPDH (relative density) $\pm$ SEM. $^*p < 0.01$ compared with the non-stretched control group.

A

C

B
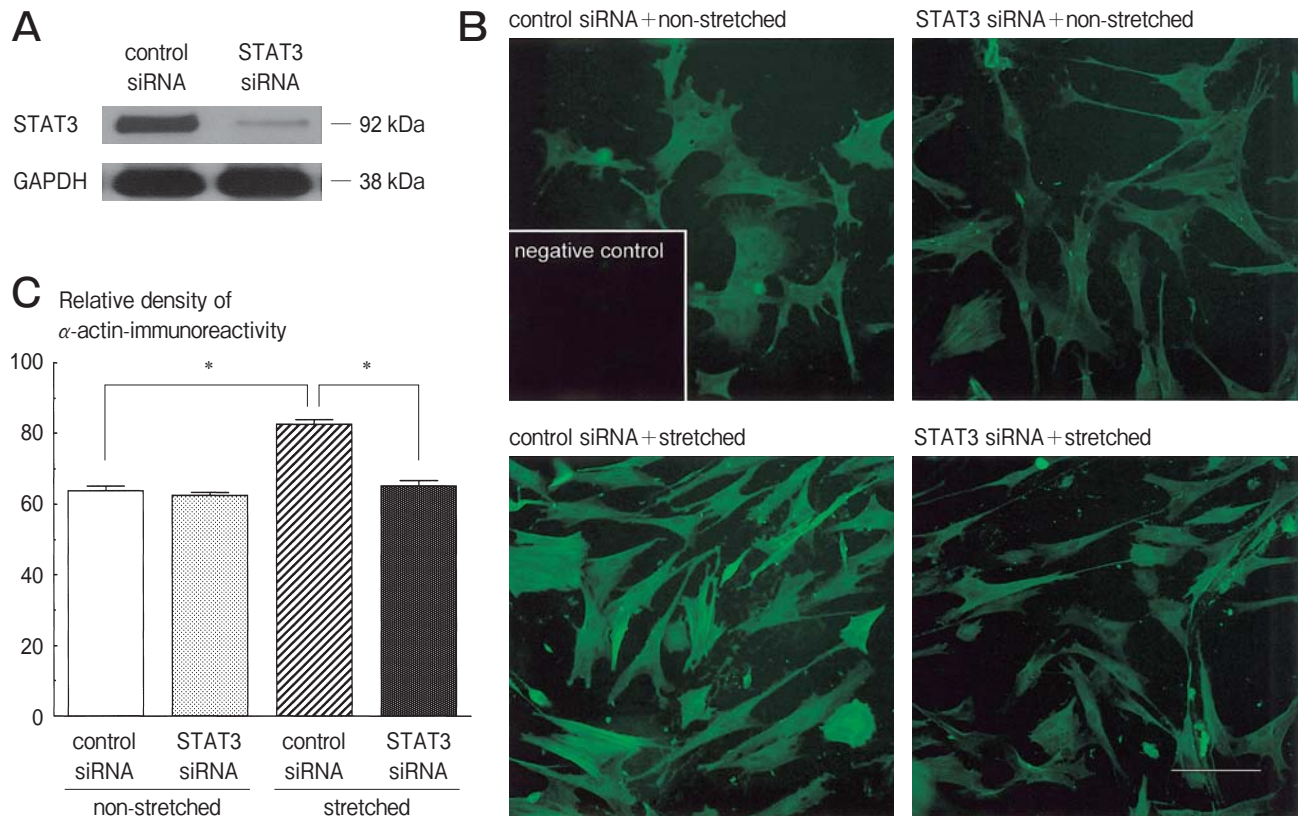
Fig. 4   Effects of transfection of siRNA for STAT3 on increases in α-smooth muscle actin expression induced by a 24-h stretch in primary cultured bladder smooth muscle cells. Western blot analyses confirm the marked reduction of STAT3 expression by the transfection with STAT3 siRNA but not with scrambled control siRNA (**A**). Immunofluorescence staining for α-smooth muscle actin after the 24-h cyclical stretch and the effects of pretreatment with siRNA for STAT3 (**B**). Negative control means staining without the primary antibody. Scale bar $= 50\,\mu$m. Relative density of fluorescence signals for α-smooth muscle actin (**C**). Data are shown as means of relative density $\pm$ SEM. $^*p < 0.01$ between the 2 indicated groups.

Discussion

The present study was designed to provide a profile of BOO induced protein expression in the rat bladder smooth muscle by using an antibody microarray. BOO induced protein expression of 64 kinds of molecules, including transcription factors, cell cycle-regulatory proteins, apoptosis-associated proteins, cytoskeletal proteins, adhesion molecules, growth factor- and stress-related proteins, signal transduction-related proteins, and nitric oxide-related proteins in the bladder tissue. Among those molecules up-regulated by BOO detected by the antibody microarray, previous studies showed increases in the expression of some molecules in the bladder smooth muscle after BOO; these molecules are related to NF-κB [2] or COX-2 [4]. Several studies indicate that the transcription factor, activator protein-1 (AP-1), is involved in the development of bladder smooth muscle hypertrophy [2, 9, 10]. In this microarray analysis, AP-1 was also up-regulated (INR = 1.25). In the profiling study using an antibody microarray, we newly found a marked increase in the expression of acute phase response factor STAT3 in rat bladder tissue after the BOO operation, which was confirmed by Western blot analysis.

STAT3 was originally identified as a molecule responsible for cytokine signaling in the interleukin-6 family system [11]. Stimulation of glycoprotein 130 (gp130), a common subunit of the interleukin-6 family cytokine receptor, leads to activation of JNK, which phosphorylates STAT3 on the tyrosine residue. It was reported that STAT3 plays a crucial role in the regeneration or remodeling of tissue *in vivo* [12]. In cardiac myocytes, the STAT3 signaling pathway is activated by extracellular stress, including catecholamine stress and mechanical stretching [13]. Recent studies show that the expression of STAT3 in cardiomyocytes regulates cardiac hypertrophy and angiogenesis [14]. The present results clearly show that STAT3 expression, especially activated phosphorylated STAT3, was induced in the bladder smooth muscle after the BOO model *in vivo*.

BOO leads to progressive wall distension caused by the incomplete emptying of urine, thereby resulting in increased local stretching of bladder smooth muscle cells. Mechanical stretch stress is thought to trigger responses in the overloaded bladder. Several studies using an *in vitro* model of mechanical stress demonstrate that repetitive stretch stimulation of bladder smooth muscle cells results in increased expression of a variety of growth factors and other specific proteins [15, 16]. The suitable conditions for mechanical stretching remain unclear. In this study, we identified the increase of STAT3 expression, consistent with the BOO *in vivo* model, at 1 Hz and 20% elongation, which indicated faster stimulation than was found in previous reports [2, 16]. To identify a mechanistic link between mechanical stimulation and growth of the bladder muscle, some groups have investigated the expression of known smooth muscle cell mitogens and other growth regulatory molecules in bladder smooth muscle cells following overdistension secondary to bladder outlet obstruction *in vivo* or in repetitive mechanical stimulation *in vitro* [9, 17]. Adam *et al.* reported that mechanical stimulation of bladder smooth muscle cells *in vitro* and whole bladder distension *ex vivo* resulted in qualitatively similar patterns of gene expression [9]. We confirmed the elevation in STAT3 expression in cultured bladder smooth muscle cells during the stress of cyclical stretching. Furthermore, we examined the correlation between STAT3 expression and the development of bladder smooth muscle hypertrophy, corresponding to the expression of a smooth-muscle-specific marker, α-smooth muscle actin, with or without the blockade of STAT3 expression using siRNA. The siRNA is a short, double-stranded RNA molecule that can target complementary mRNA for degradation via a cellular process termed RNA interference [18]. Recently, siRNA has emerged as a powerful RNAi reagent for directed posttranscriptional gene silencing and inhibition of viral propagation [19]. In the present study, we demonstrated that the blockade of STAT3 expression by the STAT3 siRNA suppresses bladder smooth muscle hypertrophy, representing an increase in α-smooth muscle actin expression following mechanical stretch stress. The present results provide evidence that STAT3 signaling may play an important role in the induction of bladder smooth muscle hypertrophy. Further studies to understand the molecular biology related to STAT3 following BOO could lead to an effective gene-modulating therapy for obstructed bladder.

References

1. Roehrborn CG and McConnell JD: Etiology, pathophysiology, epidemiology, and natural history of benign prostatic hyperplasia; in Campbell's Urology, Walsh PC, Retik AB, Vaughan EDJ and Wein AJ eds, 8 th ED, WB Saunders, Philadelphia (2002) pp 1297–1336.

2. Persson K, Dean-Mckinney T, Steers WD and Tuttle JB: Activation of the transcription factors nuclear factor-kappaB and activator protein-1 in bladder smooth muscle exposed to outlet obstruction and mechanical stretching. J Urol (2001) 165: 633–639.

3. Kushida N, Kabuyama Y, Yamaguchi O and Homma Y: Essential role for extracellular Ca(2 +) in JNK activation by mechanical stretch in bladder smooth muscle cells. Am J Physiol Cell Physiol (2001) 281: C1165–1172.

4. Park JM, Yang T, Arend LJ, Smart AM, Schnermann JB and Briggs JP: Cyclooxygenase-2 is expressed in bladder during fetal development and stimulated by outlet obstruction. Am J Physiol (1997) 273: F538–544.

5. Buttyan R, Chen MW and Levin RM: Animal models of bladder outlet obstruction and molecular insights into the basis for the development of bladder dysfunction. Eur Urol (1997) 32: 32–39.

6. Nozaki K, Tomizawa K, Yokoyama T, Kumon H and Matsui H: Calcineurin mediates bladder smooth muscle hypertrophy after bladder outlet obstruction. J Urol (2003) 170: 2077–2081.

7. Nielsen UB, Cardone MH, Sinskey AJ, MacBeath G and Sorger PK: Profiling receptor tyrosine kinase activation by using Ab microarrays. Proc Natl Acad Sci USA (2003) 100: 9330–9335.

8. Laemmli UK: Cleavage of structural proteins during the assembly of the head of bacteriophage. T4. Nature (1970) 227: 680–685.

9. Adam RM, Eaton SH, Estrada C, Nimgaonkar A, Shih SC, Smith LE, Kohane IS, Bagli D and Freeman MR: Mechanical stretch is a highly selective regulator of gene expression in human bladder smooth muscle cells. Physiol Genomics (2004) 20: 36–44.

10. Yamaguchi O: Response of bladder smooth muscle cells to obstruction: signal transduction and the role of mechanosensors. Urology (2004) 63: 11–16.

11. Kishimoto T, Taga T and Akira S: Cytokine signal transduction. Cell (1994) 76: 253–262.

12. Sano S, Itami S, Takeda K, Tarutani M, Yamaguchi Y, Miura H, Yoshikawa K, Akira S and Takeda J: Keratinocyte-specific ablation of Stat3 exhibits impaired skin remodeling, but does not affect skin morphogenesis. EMBO (1999) 18: 4657–4668.

13. Pan J, Fukuda K, Saito M, Matsuzaki J, Kodama H, Sano M, Takahashi T, Kato T and Ogawa S: Mechanical stretch activates the JAK/STAT pathway in rat cardiomyocytes. Circ Res (1999) 84: 1127–1136.

14. Osugi T, Oshima Y, Fujio Y, Funamoto M, Yamashita A, Negoro M, Kunisada S, Izumi K, Nakaoka Y, Hirota H, Okabe M, Yamauchi-Takihara K, Kawase I and Kishimoto T: Cardiac-specific activation of signal transducer and activator of transcription 3 promotes vascular formation in the heart. J Biol Chem (2002) 277: 6676–6681.

15. Orsola A, Adam RM, Peters CA and Freeman MR: The decision to undergo DNA or protein synthesis is determined by the degree of mechanical deformation in human bladder muscle cells. Urology (2002) 59: 779–783.

16. Galvin DJ, Watson RW, Gillespie JI, Brady H and Fitzpatrick JM: Mechanical stretch regulates cell survival in human bladder smooth muscle cells in vitro. Am J Physiol Renal Physiol (2002) 283: F1192–1199.

17. Chaqour B, Whitbeck C, Han JS, Macarak E, Horan P, Chichester P and Levin R: Cyr61 and CTGF are molecular markers of bladder wall remodeling after outlet obstruction. Am J Physiol Endocrinol Metab (2002) 283: E765–774.

18. Zamore PD, Tuschl T, Sharp PA and Bartel DP: RNAi: double-stranded RNA directs the ATP-dependent cleavage of mRNA at 21 to 23 nucleotide intervals. Cell (2000) 101: 25–33.

19. Wilson JA, Jayasena S, Khvorova A, Sabatinos S, Rodrigue-Gervais IG, Arya S, Sarangi F, Harris-Brandts M, Beaulieu S and Richardson CD: RNA interference blocks gene expression and RNA synthesis from hepatitis C replicons propagated in human liver cells. Proc Natl Acad Sci USA (2003) 100: 2783–2788.

Erratum

In the article by **Fujita O.**, *et al.* entitled "**Involvement of STAT3 in Bladder Smooth Muscle Hypertrophy Following Bladder Outlet Obstruction**", which appeared in the **December 2006** issue, **Vol. 60**, **No. 6**, **pp 299–309**, a correction should be noted in the last line of *Western blot analysis* on page 301.

Error:

reacted with donkey anti-mouse IgG (Chemicon).

Correction:

reacted with donkey anti-mouse IgG (Chemicon) or donkey anti-rabbit IgG secondary antibodies (Amersham Biosciences) at room temperature for 1h. Specific signals of proteins were visualized by chemiluminescence using the ECL Western blotting detection kit (Amersham Biosciences). The relative density of detected signals on the blots was measured and analyzed with image scanner and image analysis software (NIH image 1.56). For quantitative analysis, the ratio for detected protein (relative density) and the constitutively expressed GAPDH protein was calculated to normalize for loading and transfer of artifacts introduced in Western blotting.